RESEARCH ARTICLE

Single-Crystal-to-Single-Crystal Installation of $Ln_4(OH)_4$ Cubanes in an Anionic Metallosupramolecular Framework

Nobuto Yoshinari,[a] Natthaya Meundaeng,[a,b] Hiroyasu Tabe,[c] Yusuke Yamada,[c] Satoshi Yamashita,[a] Yasuhiro Nakazawa,[a] Takumi Konno*[a]

[a] Dr. N. Yoshinari, Dr N. Meundaeng, Dr. S. Yamashita, Prof Y. Nakazawa, Prof T. Konno
Department of Chemistry, Graduate School of Science,
Osaka University
Toyonaka, Osaka 560-0043 (JAPAN)
E-mail: konno@chem.sci.osaka-u.ac.jp
[b] Dr N. Meundaeng,
Department of Chemistry, Faculty of Science,
King Mongkut's Institute of Technology Ladkrabang
Bangkok, 10520 (THAILAND)
[c] Dr. H. Tabe, Prof. Y. Yamada
Graduate School of Engineering,
Osaka City University
Sugimoto, Sumiyoshi, Osaka 558-8585 (JAPAN)

Supporting information for this article is given via a link at the end of the document.

Abstract: Here, we report the first example of the postsynthetic installation of lanthanide cubanes into a metallosupramolecular framework via a single-crystal-to-single-crystal (SCSC) transformation. Soaking single crystals of $K_6[Rh_4Zn_4O(L\text{-cys})_{12}]$ (K_6[**1**]; L-H_2cys = L-cysteine) in a water/ethanol solution containing $Ln(OAc)_3$ (Ln^{3+} = lanthanide ion) results in the exchange of K^+ by Ln^{3+} with retention of the single crystallinity, producing Ln_2[**1**] (**2**$_{Ln}$) and $Ln_{0.33}[Ln_4(OH)_4(OAc)_3(H_2O)_7]$[**1**] (**3**$_{Ln}$) for early and late lanthanides, respectively. While the Ln^{3+} ions in **2**$_{Ln}$ exist as disordered aqua species, those in **3**$_{Ln}$ form ordered hydroxide-bridged cubane clusters that connect [**1**]$^{6-}$ anions in a 3D metal-organic framework through coordination bonds with carboxylate groups. This study shows the utility of an anionic metallosupramolecular framework with carboxylate groups for the straightforward, systematic creation of a series of metal cubanes that have great potential for various applications, such as magnetic materials and heterogeneous catalysts.

Introduction

The postsynthetic modification (PSM) of crystalline solids has attracted the attention of synthetic chemists and material scientists for a long time.[1-4] This is because PSM allows the creation of new compounds and materials that are difficult to synthesize via conventional methods.[1-3] Recently, functional host-guest composite materials have been created using the PSM approach.[4,5] The initial development of PSM started with porous inorganic materials, represented by zeolites.[2] Subsequently, it was applied to metal-organic frameworks (MOFs), which are porous materials with infinite coordination-bonding networks.[3] It has been shown that the robustness of MOFs allows small molecules or ions to penetrate their interstices, leading to metal or ligand exchange, ligand modification, and the incorporation and fabrication of metal complexes or clusters in the interstices.[3-5] In contrast to the development of PSMs in infinite porous materials, PSMs of crystalline metallosupramolecular compounds consisting of discrete molecules or ions are much less explored, mainly due to the inherent weakness of their frameworks, which consist of noncovalent interactions.[6] The limited examples involve (i) the exchange of counterions or solvents,[7] (ii) the condensation of guest molecules or ions,[8,9] and (iii) the coordination of guest molecules or ions to host metal centers.[10,11]

Lanthanide clusters with bridging hydroxide groups have received increasing attention. To date, a variety of clusters of $Ln_x(OH)_y$ with different compositions that show intriguing photophysical, magnetic, and catalytic properties, have been synthesized by using O- or N-donating ancillary ligands.[12-15] However, the isolation of this class of clusters in a controlled manner is quite difficult due to the large pH dependency,[13] as well as the geometrical flexibility of lanthanide ions.[16] PSM is expected to provide a promising approach to synthesizing lanthanide hydroxide clusters, given that the spatial constraint of the crystal framework of the host prevents the random growth of cluster structures. In this work, we report that lanthanide hydroxide clusters are created in an anionic metallosupramolecular framework via the PSM approach. As a crystalline host compound, we employed the ionic solid $K_6[Rh_4Zn_4O(L\text{-cys})_{12}]$ (K_6[**1**]; L-cys = L-cysteinate) bearing free carboxylate groups, which shows superionic conduction due to the hydrated K^+ ions at room temperature.[17,18] Just by soaking crystals of K_6[**1**] in a solution containing $Ln(OAc)_3$, the K^+ ions in K_6[**1**] were replaced by Ln^{3+} ions to form new crystalline products, **2**$_{Ln}$ and **3**$_{Ln}$, for early lanthanides (La^{III}, Ce^{III}, Pr^{III}, Nd^{III}, Sm^{III}, and Eu^{III}) and late lanthanides (Gd^{III}, Tb^{III}, Dy^{III}, Er^{III}, Ho^{III}, Tm^{III}, Yb^{III}, and Lu^{III}), respectively, in a single-crystal-to-single-crystal (SCSC) transformation manner (Scheme 1). Crystalline **2**$_{Ln}$ was found to contain disordered aqua Ln^{3+} ions, most of which bind to [**1**]$^{6-}$ anions through coordination bonds. Remarkably, Ln^{3+} ions in **3**$_{Ln}$ were found to form tetranuclear cubane clusters, $[Ln_4(\mu_3\text{-}OH)_4(\mu_2\text{-}OAc)_3(H_2O)_7]^{5+}$, which connect [**1**]$^{6-}$ anions in a 3D MOF structure through coordination bonds. The creation of such a series of lanthanide cubanes via an SCSC process, as well as the SCSC transformation of an ionic solid to a MOF structure by the exchange of counter cations, is unprecedented.

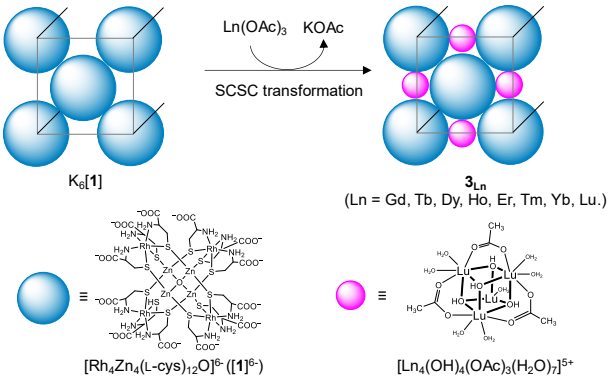

Scheme 1. Postsynthetic installation of $Ln_4(OH)_4$ cubane clusters in the $[\mathbf{1}]^{6-}$ framework.

Results and Discussion

Synthesis, characterization, and structure of $\mathbf{2_{La}}$.

Freshly prepared single crystals of $K_6[\mathbf{1}]$ ($K_6[Rh_4Zn_4O(L\text{-cys})_{12}]$) with a rhombic-dodecahedron shape (0.1 - 0.2 mm) were soaked in a 0.02 M solution of $La(OAc)_3$ in water/ethanol (1:3) for one week. To complete the reaction, the solution was changed to a 0.1 aqueous solution of $La(OAc)_3$, and the crystals were soaked for an additional few days. While crystals of $K_6[\mathbf{1}]$ are highly soluble in water, the resulting crystals ($\mathbf{2_{La}}$) are insoluble in water although their crystal shape, size, and color do not change (Fig. S1),[19] which is indicative of the SCSC transformation from $K_6[\mathbf{1}]$ to $\mathbf{2_{La}}$. The retention of the S-bridged $Rh^{III}_4Zn^{II}_4$ octanuclear structure in $[\mathbf{1}]^{6-}$ in the course of the reaction was confirmed by the infrared (IR) and diffuse reflectance (DR) spectra of $\mathbf{2_{La}}$ in the solid-state, which are essentially the same as those of $K_6[\mathbf{1}]$ (Figs. S2 and S3).[19] X-ray fluorescence (XRF) analysis showed that $\mathbf{2_{La}}$ contains La, Rh, and Zn atoms as metal components in a 1:2:2 ratio, and K atoms were not detected.[19]

Single-crystal X-ray (SCXR) analysis revealed that the crystals of $\mathbf{2_{La}}$ belong to the cubic space group $P2_13$, which is the same as that of $K_6[\mathbf{1}]$.[18a,19] Consistent with this, no significant differences in the powder X-ray diffraction (PXRD) patterns of $K_6[\mathbf{1}]$ and $\mathbf{2_{La}}$ were observed (Fig. S4).[19] As shown in Fig. 1a, $\mathbf{2_{La}}$ contains $[\mathbf{1}]^{6-}$ complex-anions with 12 coordinated amine and 12 pendent carboxylate groups on its spherical surface. In $\mathbf{2_{La}}$, each complex-anion is linked to six neighboring complex-anions through NH···O hydrogen bonds (Figs. 1b), forming a 3D hydrogen-bonding network with a **lcy**-type topology (Fig. 1c).[17b,20] While this network is the same as that in $K_6[\mathbf{1}]$, the hydrogen bonds in $\mathbf{2_{La}}$ (2.87-2.98 Å) are longer than those in $K_6[\mathbf{1}]$ (2.75-2.91 Å).[18a] Two aqua La^{3+} ions, which are positionally disordered in four positions (La1A, La1A, La2A, and La2A), are present per $[\mathbf{1}]^{6-}$ complex-anion in $\mathbf{2_{La}}$, consistent with its chemical formula of $La_2[\mathbf{1}]\cdot nH_2O$, which was determined based on elemental analysis, although the water molecules bound to La^{3+} ions were not fully located due to severe disorder.[21] In an interstitial space of the hydrogen-bonding framework in $\mathbf{2_{La}}$ (site A), the La1B atom is located on the crystallographic C_3 axis and is surrounded by the three disordered La1A atoms that are coordinated to three carboxylate groups from three $[\mathbf{1}]^{6-}$ complex-anions (Fig. 1d). In another interstitial space (site B), both the disordered La2A and La2B atoms are coordinated to carboxylate groups and are located around the C_3 axis (Fig. S5).[19] Thus, $\mathbf{2_{La}}$ can be described as an ionic crystal with a hydrogen-bonding framework made up of $[\mathbf{1}]^{6-}$ anions, the interstitial spaces of which accommodate aqua La^{3+} ions to balance the charge of the crystal (Fig. S6).[19]

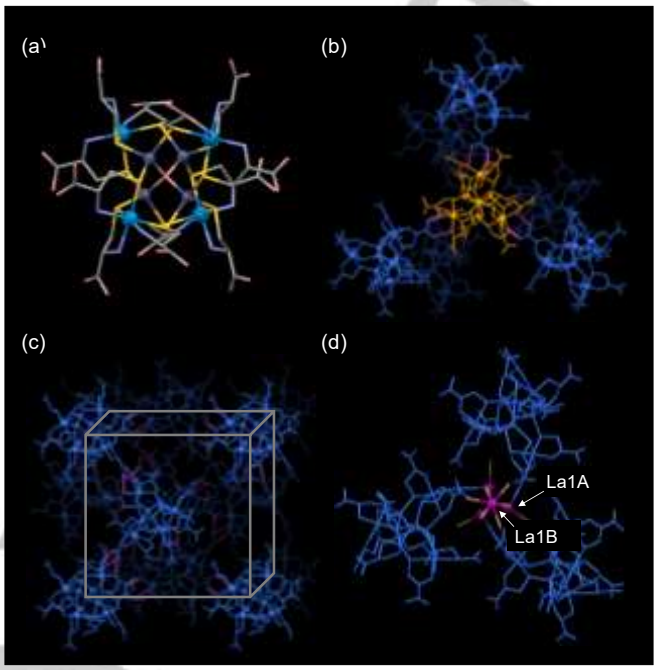

Figure 1. Perspective views of (a) the molecular structure of $[\mathbf{1}]^{6-}$, (b) $[\mathbf{1}]^{6-}$ anion (yellow) hydrogen-bonded to six adjacent $[\mathbf{1}]^{6-}$ anions (blue), (c) the hydrogen-bonded framework composed of $[\mathbf{1}]^{6-}$ anions (blue), and (d) the disordered aqua La ions at site A in $\mathbf{2_{La}}$. H atoms have been omitted for clarity. Color code: La: red-purple; Rh, blue; Zn, dark gray; S, yellow; O, pink; N, pale blue; C, gray. Dashed pink lines indicate H bonds.

Synthesis, characterization, and structure of $\mathbf{3_{Lu}}$.

The same treatment using $Lu(OAc)_3$ instead of $La(OAc)_3$ also gave water-insoluble crystals ($\mathbf{3_{Lu}}$) via SCSC transformation. While the IR and DR spectral features of $\mathbf{3_{Lu}}$ are the same as those of $\mathbf{2_{La}}$ (Figs. S2 and S3),[19] XRF analysis indicated that $\mathbf{3_{Lu}}$ contains Lu, Rh, and Zn atoms in a 1:1:1 ratio, rather than the 1:2:2 ratio seen in $\mathbf{2_{La}}$. In addition, the intensity ratios of the diffractions in the PXRD profile of $\mathbf{3_{Lu}}$ are different from those of $\mathbf{2_{La}}$, especially for the (111) and (200) indices (Fig. S4).[19] Single-crystal X-ray analysis indicated that crystals of $\mathbf{3_{Lu}}$ also belong to the cubic space group $P2_13$, forming a 3D hydrogen-bonding framework analogous to that of $\mathbf{2_{La}}$ (Fig. S7).[19] In addition, the N-H···O hydrogen bonds in $\mathbf{3_{Lu}}$ (2.85-2.98 Å) are similar to those in $\mathbf{2_{La}}$ (2.87-2.98 Å), despite the much smaller ionic radius of Lu^{3+} (0.86 Å) compared with that of La^{3+} (1.03 Å).[16] Notably, in each interstitial space corresponding to site A in $\mathbf{2_{La}}$, the incorporated Lu^{3+} ions in $\mathbf{3_{Lu}}$ form a tetranuclear $[Lu_4(OH)_4(OAc)_3(H_2O)_7]^{5+}$ cluster (Fig. 2a) with four Lu^{3+} atoms spanned by four μ_3-OH^- ions in a tetrahedral geometry to form a cubane-type $\{Lu_4(OH)_4\}^{8+}$ core.[21] The intracluster Lu···Lu distances (av. 3.68 Å) in $\mathbf{3_{Lu}}$, as well as the Lu–O bond distances (av. 2.31 Å), are similar to those in discrete $[Lu_4(OH)_4(FcacacPh)_8]$ (av. Lu···Lu = 3.65 Å, av. Lu–O = 2.30 Å),[22] which is the only example of a lutetium hydroxide cubane cluster reported thus far. In each cubane cluster of $\mathbf{3_{Lu}}$, the three pairs of Lu^{III} centers (Ln2···Ln2) in the trigonal basal

plane of the Lu^{III}_4 tetrahedron are each spanned by an acetate ion (av. Lu–O_{OAc} = 2.26 Å), which appears to maintain the cubane structure. In addition, the remaining three pairs of Lu^{III} centers (Ln1···Ln2) are each spanned by a carboxylate group of [**1**]$^{6-}$ (Lu–O_{COO} = 2.26 Å). Thus, each cubane cluster connects three [**1**]$^{6-}$ anions through carboxylate groups such that each [**1**]$^{6-}$ anion is surrounded by three cubane clusters (Figs 2b and 2c). As a result, the cubane cations and the [**1**]$^{6-}$ anions are alternately linked by COO-Lu coordination bonds to construct a 3D MOF structure with **srs-b**-type topology in **3$_{Lu}$** (Fig. 2d).[20] In the cubane cluster of **3$_{Lu}$**, the Lu1 and Lu2 centers are coordinated by one and two water molecules, in addition to carboxylate and hydroxide groups, completing 7-coordinate face-capped octahedron and 8-coordinated dodecahedron (Lu2) geometries, respectively (Fig. 2a).[23] To balance the charge of the crystal, disordered Lu^{3+} ions (Lu3A and Lu3B) exist in interstitial spaces corresponding to site B and another site C in **2$_{La}$** (Fig. S8).[19] In addition, the interstices of the MOF structure in **3$_{Lu}$** are occupied by a number of water molecules of crystallization (Fig. S9).[19,24] Thus, the formula of **3$_{Lu}$** is represented as $Lu_{0.33}$[{$Ln_4(OH)_4(OAc)_3(H_2O)_7$}{**1**}]·$nH_2O$, which agrees well with the elemental analysis.

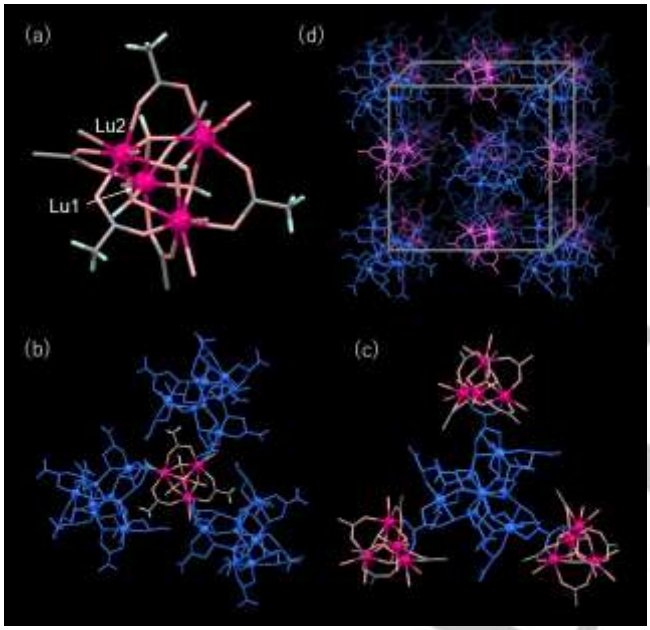

Figure 2. Perspective views of (a) the Lu^{III}_4 cubane cluster, (b) the Lu_4 cubane cluster connected to three [**1**]$^{6-}$ (blue), (c) [**1**]$^{6-}$ bound to three Lu_4 cubane clusters, and (d) the packing structure in **3$_{Lu}$**. H atoms except for cubane clusters in (a) and (b) have been omitted for clarity. Color code: Lu: dark red purple; O, pink; C, gray; H: light blue.

Synthesis, characterization, and structures of 2$_{Ln}$ and 3$_{Lu}$.

Prompted by the production of **2$_{La}$** and **3$_{Gd}$** with $La(OAc)_3$ and $Lu(OAc)_3$, respectively, crystals of K_6[**1**] were immersed in an aqueous ethanol solution containing other $Ln(OAc)_3$ species (Ln = Ce, Pr, Nd, Sm, Eu, Gd, Tb, Dy, Ho, Er, Tm, and Yb) under the same conditions. As expected, this treatment led to the complete exchange of K^+ ions in K_6[**1**] by Ln^{3+} ions, producing crystals of **2$_{Ln}$** (Ln = Ce, Pr, Nd, Sm, and Eu) and **3$_{Ln}$** (Ln = Gd, Tb, Dy, Ho, Er, Tm, and Yb) via an SCSC process. The XRF and elemental analyses indicated that **2$_{Ce}$**, **2$_{Pr}$**, **2$_{Nd}$**, **2$_{Sm}$**, and **2$_{Eu}$** with early lanthanides and **3$_{Gd}$**, **3$_{Tb}$**, **3$_{Dy}$**, **3$_{Ho}$**, **3$_{Er}$**, **3$_{Tm}$**, and **3$_{Yb}$** with late lanthanides have the same formulas as those of **2$_{La}$** and **3$_{Lu}$**, respectively. In addition, the former and the latter products show PXRD features that are essentially the same as those of **2$_{La}$** and **3$_{Lu}$**, respectively (Fig. S10).[19] Single-crystal X-ray analysis established that **2$_{Ln}$** (Ln = Ce, Pr, Nd, Sm, and Eu) and **3$_{Ln}$** (Ln = Gd, Tb, Dy, Ho, Er, Tm, and Yb) are isostructural with **2$_{La}$** and **3$_{Lu}$**, respectively, possessing the ionic solid structure of Ln_2[**1**]·nH_2O (Fig. S11) and the 3D MOF structure of $Ln_{0.33}$[{$Ln_4(OH)_4(OAc)_3(H_2O)_7$}{**1**}]·$nH_2O$ (Figs. 3 and S12), respectively.[19] In **3$_{Ln}$**, the averaged Ln···Ln distances in the $\{Ln_4(OH)_4\}^{8+}$ cubanes decrease in the order **3$_{Gd}$** (3.81 Å) > **3$_{Tb}$** (3.79 Å) > **3$_{Dy}$** (3.77 Å) > **3$_{Ho}$** (3.75 Å) > **3$_{Er}$**, **3$_{Tm}$** (3.73 Å) > **3$_{Yb}$** (3.69 Å) > **3$_{Lu}$** (3.68 Å), in parallel with the decrease in the ionic radii of Ln^{3+} due to 'lanthanide contraction'.[16] It appears that the interstitial space surrounded by three [**1**]$^{3-}$ anions in the hydrogen-bonding framework is not large enough to accommodate the $\{Ln_4(OH)_4\}^{8+}$ cubanes containing early lanthanide ions with larger ionic radii, with the border existing between Eu^{3+} and Gd^{3+} ions.[25] Thus, the lanthanide ions in **2$_{La}$**, **2$_{Ce}$**, **2$_{Pr}$**, **2$_{Nd}$**, **2$_{Sm}$**, and **2$_{Eu}$** are located in the interstitial spaces as disordered aqua species, without forming $\{Ln_4(OH)_4\}^{8+}$ cubane clusters. Note that the direct reactions of $Ln(OAc)_3$ and K_6[**1**] in aqueous media resulted in the precipitation of amorphous solids containing Ln^{3+} and [**1**]$^{6-}$ in a 2:1 ratio. This result indicates that the interstitial spaces in the hydrogen-bonding framework act as a template available for creating lanthanide clusters. Such a template effect due to interstitial spaces has not been reported in discrete supramolecular systems to date.

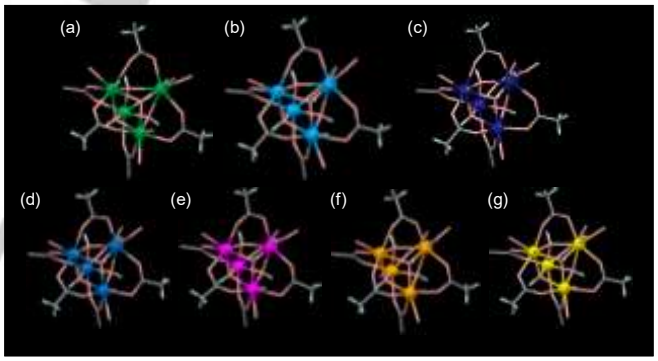

Figure 3. Perspective views of the $Ln_4(OH)_4$ clusters in (a) **3$_{Gd}$**, (b) **3$_{Tb}$**, (c) **3$_{Dy}$**, (d) **3$_{Ho}$**, (e) **3$_{Er}$**, (f) **3$_{Tm}$**, (g) and **3$_{Yb}$**.

Magnetic properties of 3$_{Ln}$.

To determine whether magnetic interactions exist between the Ln^{3+} centers in the $\{Ln_4(OH)_4\}^{8+}$ cubane, temperature-dependent magnetic susceptibility measurements (H = 1000 Oe, T = 2-300 K) were performed for **3$_{Ln}$** (Fig. 4a). At 300 K, these compounds gave $\chi_M T$ values (cm^3Kmol^{-1}) of 30.5 (**3$_{Gd}$**), 44.1 (**3$_{Tb}$**), 49.7 (**3$_{Dy}$**), 53.0 (**3$_{Ho}$**), 41.6 (**3$_{Er}$**), 21.7 (**3$_{Tm}$**), and 9.58 (**3$_{Yb}$**), which are similar to the expected values for the four isolated Ln^{3+} ions (31.5 for Gd^{III}_4, 47.2 for Tb^{III}_4, 56.4 for Dy^{III}_4, 56.2 for Ho^{III}_4, 45.9 for Er^{III}_4, 28.6 for Tm^{III}_4, and 10.3 for Yb^{III}_4).[26] The magnetic features of these compounds are consistent with previous reports that show the absence of magnetic interaction between Ln^{3+} centers in cubane-type lanthanide clusters.[15,27] We also investigated the molar magnetocaloric effects due to lanthanide ions using **3$_{Gd}$**, considering that the Gd^{3+} has the largest spin value (7/2) among

lanthanide ions.[16,25] The $-\Delta S_m^{max}$ value for **3Gd** was evaluated to be 46 $JK^{-1}mol^{-1}$ (Fig. S13).[19] This value is comparable with that reported for $[Gd_4(OH)_4(C_2O_4)(H_2O)_5(SO_4)_3]$ having a $\{Gd_4(OH)_4\}^{8+}$ cubane core (60 $JK^{-1}mol^{-1}$).[28] With this result in hand, we subjected a pelletized sample (1.1 mg) of **3Gd** to an external magnetic field of 5 T at 2.6 K to investigate the magnetic cooling ability of **3Gd**. When the magnetic field was reduced from 5 T to 2 T, drastic cooling from 2.6 K to 1.8 K was observed (Fig. 4b). Further cooling was not observed even when the magnetic field was reduced from 2 T to 0 T. On the other hand, increasing the magnetic field from 0 T to 3 T resulted in the temperature of the sample increasing by 0.6 K. Thus, **3Gd** can be used as a magnetic cooling material that can cool below 2 K under magnetic fields of 2-5 T. Note that this is the first experimental evidence of a magnetic cooling effect due to $\{Gd_4(OH)_4\}^{8+}$ cubane.

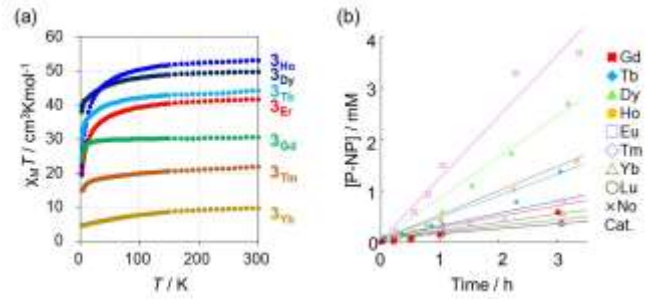

Figure 4. (a) The $\chi_M T$ versus T plots of **3Ln** (H = 1000 Oe). (b) The catalytic hydrolysis of *p*-nitrophenyl phosphate (*p*-NPP) by **3Ln** under heterogeneous conditions.

Catalytic activities of 3Ln.

Catalytic hydrolysis is one of the most attractive applications of lanthanide clusters.[29] Nevertheless, reports on the heterogeneous catalytic activity of lanthanide clusters are very rare.[30] We examined the catalytic hydrolysis of a phosphate ester as a representative example of Lewis acid catalysis. The crystals of **3Ln** (3.0 mg) were soaked in an aqueous buffer solution (100 mM, pH 8.3) containing *p*-nitrophenyl phosphate (*p*-NPP, 25 mM) as the substrate (Fig. 5a). During the reaction, *p*-NPP was decomposed into *p*-nitrophenolate (*p*-NP) and phosphate by the hydrolysis reaction, which was monitored by a UV-Vis spectrophotometer (Fig. 5b).[19,31] As illustrated in Fig. 5c, the catalytic activities of **3Ln** vary depending on the type of Ln^{3+} in the compound. It is common that the activities increase going from Gd^{3+} to Lu^{3+}, as their Lewis acidities increase due to the contraction of the ionic radii.[16] This is also the case for the present system from **3Gd** to **3Er**. However, the activities decrease from **3Er** to **3Lu**, with **3Lu** showing the lowest activity in this system. It is assumed that large lanthanide ions can expand the gate of the framework to a greater extent, which allows the substance to approach the catalytic Ln^{3+} centers inside the crystal more easily. Thus, the unusual trend in the catalytic activities of **3Ln** results from the balance between the gate sizes of the framework and the Lewis acidities of the Ln^{3+} ions. This is the first report that shows the heterogeneous catalytic activities of a series of lanthanide-cubane clusters installed in MOFs.

Conclusion

We found in this study that the K^+ ions in K_6[**1**] are easily completely exchanged by Ln^{3+} ions in the SCSC manner when soaking its crystals in aqueous ethanol containing $Ln(OAc)_3$. Of note is the formation of hydroxide-bridged lanthanide cubanes that connect $[\mathbf{1}]^{6-}$ anions in the 3D MOF structure. The formation of these cubanes was dependent on the size of the Ln^{3+} ions; the MOF structure in **3Ln** was formed for later lanthanides (Gd^{3+}, Tb^{3+}, Dy^{3+}, Er^{3+}, Ho^{3+}, Tm^{3+}, Yb^{3+}, and Lu^{3+}), whereas early lanthanide ions (La^{3+}, Ce^{3+}, Pr^{3+}, Nd^{3+}, Sm^{3+}, Eu^{3+}) gave ionic solid structures in **2Ln**. Thus, a series of lanthanide cubanes (Ln = Gd - Lu) with the same structure and coordination environment were created for the first time via a simple, straightforward postsynthetic modification approach. This enabled us to perform systematic investigations of the magnetic and catalytic properties of the lanthanide cubanes installed in MOF structures, demonstrating their potential applications as magnetic cooling materials and heterogeneous catalysts. Considering that the interstitial spaces surrounded by free carboxylate groups of $[\mathbf{1}]^{6-}$ function as templates for creating the lanthanide cubane clusters, the development of other ionic crystals of coordination compounds having free carboxylate groups, as well as the postsynthetic installation of transition-metal cubanes by using K_6[**1**], is currently in progress in our laboratory.

Acknowledgments

This work was supported by JST CREST (Grant No. JPMJCR13L3) and JSPS KAKENHI (Grant Nos. 19K05496 and 18H05344). The synchrotron radiation experiments were performed at Spring-8 with the approval of JASRI (Proposal Nos. 2019A1279, 2019A1302, 2019B1107, and 2019B1108) and at 2D-SMC of the Pohang Accelerator Laboratory.

Keywords: Cluster compounds • Crystal engineering • Lanthanides • Postsynthetic modification

[1] a) C. Martínez, A. Corma, *Coord. Chem. Rev.* **2011**, *255*, 1558-1580; b) J. L. Segura, S. Royuela, M. M. Ramos, *Chem. Soc. Rev.* **2019**, *48*, 3903-3945.

[2] V. Valtchev, G. Majano, S. Mintova, J. Pérez-Ramírez, *Chem. Soc. Rev.* **2013**, *42*, 263-290.

[3] a) Z. Wang, S. M. Cohen, *Chem. Soc. Rev.* **2009**, *38*, 1315-1329; b) S. M. Cohen, *Chem. Rev.* **2012**, *112*, 970-1000; c) M. Lalonde, W. Bury, O. Karagiaridi, Z. Brown, J. T. Hupp, O. K. Farha, *J. Mater. Chem. A* **2013**, *1*, 5453; d) C. K. Brozek, M. Dinca, *Chem. Soc. Rev.* **2014**, *43*, 5456-5467; e) P. Deria, J. E. Mondloch, O. Karagiaridi, W. Bury, J. T. Hupp, O. K. Farha, *Chem. Soc. Rev.* **2014**, *43*, 896-5912; f) O. Karagiaridi, W. Bury, J. E. Mondloch, J. T. Hupp, O. K. Farha, *Angew. Chem.* **2014**, *53*, 4530-4540; g) S. M. Cohen, *J. Am. Chem. Soc.* **2017**, *139*, 2855-2863.

[4] a) J. D. Evans, C. J. Sumby, C. J. Doonan, *Chem. Soc. Rev.* **2014**, *43*, 5933-5951; b) Z. Yin, S. Wan, J. Yang, M. Kurmoo, M.-H. Zeng, *Coord. Chem. Rev.* **2019**, *378*, 500-512.

[5] a) X. Gu, Z.-H. Lu, H.-L. Jiang, T. Akita, Q. Xu, *J. Am. Chem. Soc.* **2011**, *133*, 11822; b) H.-L. Jiang, B. Liu, T. Akita, M. Haruta, H. Sakurai, Q. Xu, *J. Am. Chem. Soc.* **2009**, *131*, 11302; c) M. Müller, S. Turner, O. Lebedev, Y. Wang, G. van Tendeloo, R. Fischer, *Eur. J. Inorg. Chem.* **2011**, 1876; d) L. B. Vilhelmsen, K. S. Walton, D. S. Sholl, *J. Am. Chem. Soc.* **2012**, *134*, 12807-12816; e) T. Wang, L. Gao, J. Hou, S. J. A. Herou, J. T. Griffiths, W. Li, J. Dong, S. Gao, M.-M. Titirici, R. V. Kumar, A. K. Cheetham, X. Bao, Q. Fu, S. K. Smoukov, *Nat. Commun.* **2019**, *10*, 1340.

[6] M. W. Schneider, I. M. Oppel, A. Griffin, M. Mastalerz, *Angew. Chem. Int. Ed.* **2013**, *52*, 3611-3615.

[7] a) Y.-J. Zhang, T. Liu, S. Kanegawa, O. Sato, *J. Am. Chem. Soc.* **2009**, *131*, 7942-7943; b) L.-Z. Cai, X.-M. Jiang, Z.-J. Zhang, P.-Y. Guo, A.-P. Jin, M.-S. Wang, G.-C. Guo, *Inorg. Chem.* **2017**, *56*, 1036-1040.

[8] E. Li, K. Jie, Y. Zhou, R. Zhao, F. Huang, *J. Am. Chem. Soc.* **2018**, *140*, 15070-15079.

[9] K. Imanishi, B. Wahyudianto, T. Kojima, N. Yoshinari, T. Konno, *Chem. Eur. J.* **2020**, *26*, 1827-1833.

[10] N. Li, F. Jiang, L. Chen, X. Li, Q. Chena, M. Hong, *Chem. Commun.* **2011**, *47*, 2327-2329.

[11] a) H. Kim, M. Oh, D. Kim, J. Park, J. Seong, S. K. Kwak, M. S. Lah, *Chem. Commun.* **2015**, *51*, 3678-3681; b) J. Lee, J. H. Kwak, W. Choe, *Nat. Commun.* **2019**, *8*, 1470.

[12] X.-Y. Zheng, J. Xie, X.-J. Kong, L.-S. Long, L.-S. Zheng, *Coord. Chem. Rev.* **2019**,

[13] a) R. Wang, Z. Zheng, T. Jin, R. J. Staples, *Angew. Chem. Int. Ed.* **1999**, *38*, 1813-1815; b) R. Wang, H. Liu, M. D. Carducci, T. Jin, C. Zheng, Z. Zheng, *Inorg. Chem.* **2001**, *40*, 2743; c) Wang, R.; Selby, H. D.; Liu, H.; Carducci, M. D.; Jin, T.; Zheng, Z.; Anthis, J. W.; Staples, R. J. Inorg. Chem.; 2002, 41, 278. d) X.-J. Kong, L.-S. Long, L.-S. Zheng, R. Wang, Z. Zheng, *Inorg. Chem.* **2009**, *48*, 3268-3273.

[14] a) J. C. Plakatouras, I. Baxter, M. B. Hursthouse, K. M. A. Malik, J. McAleesea, S. R. Drake, *J. Chem. Soc., Chem. Commun.* **1994**, 2455-2456; b) B.-Q. Ma, D.-S. Zhang, S. Gao, T.-Z. Jin, C.-H. Yan, G.-X. Xu, *Angew. Chem. Int. Ed. Engl.* **2000**, *39*, 3644-3646; c) O. A. Gerasko, E. A. Mainicheva, M. I. Naumova, M. Neumaier, M. M. Kappes, S. Lebedkin, D. Fenske, V. P. Fedin, *Inorg. Chem.* **2008**, *47*, 8869-8880; d) X. Li, X.-S. Wua, X.-J. Zheng, *Inorg. Chim. Acta* **2009**, *362*, 2537-2541; e) X. Yi, K. Bernot, G. Calvez, C. Daiguebonne, O. Guillou, *Eur. J. Inorg. Chem.* **2013**, 5879-5885; f) G. Xiong, L. You, B. Ren, Y. He, S. Wang, Y. Sun, *Eur. J. Inorg. Chem.* **2016**, 3969-3977; g) H. Wu, S. Zhang, M. Li, C. Qiao, L. Sun, Q. Wei, G. Xie, S. Chen, S. Gao, *ChemistrySelect* **2016**, *1*, 3335-3342; h) L. Shen, Y.-T. Min, X. Bai, J. Wang, Q. Wu, J. Yang, H.-J. Chen, F. Geng, G.-W. Yang, Q.-Y. Li, *Z. Anorg. Allg. Chem.* **2016**, *642*, 1112-1119; i) J. D. Einkauf, J. P. Karram, N. E. Greig, B. C. Chan, D. T. Lill, *Eur. J. Inorg. Chem.* **2016**, 1085-1092; j) M. Y. Guo, L. J. Qiu, C. Y. Zhang, W. H. Guan, N. N. Feng, X. D. Hu, Q. Y. Li, G. W. Yang, *Inorg. Chim. Acta* **2016**, *453*, 583-588.

[15] Y. M. Litvinova, Y. M. Gayfulin, J. van Leusen, D. G. Samsonenko, V. A. Lazarenko, Y. V. Zubavichus, P. Kögerler, Y. V. Mironov, *Inorg. Chem. Front.* **2019**, *6*, 1518-1526.

[16] *Lanthanide and Actinide Chemistry* (Ed. S. Cotton), Wiley, Chichester, **2006**.

[17] a) T. Konno, K. Okamoto, J. Hidaka, *Inorg. Chem.* **1994**, *33*, 538-544; b) N. Yoshinari, U. Yamashita, T. Konno, *CrystEngComm*, **2013**, *15*, 10016-10019.

[18] a) N. Yoshinari, S. Yamashita, Y. Fukuda, Y. Nakazawa, T. Konno, *Chem. Sci.* **2019**, *10*, 587-593; b) N. Yoshinari, T. Konno, *Molecular Technology, Vol. 4: Synthesis Innovation*, (Ed. H. Yamamoto, T. Kato), Wiley-VCH, Weinheim, Germany, 2019, pp. 199–230.

[19] See the supporting information.

[20] a) O. D. Friedrichs, M. O'Keeffe, O. M. Yaghi, *Acta Cryst.* **2003**, *A59*, 515-525; b) M. O'Keeffe, M. A. Peskov, S. J. Ramsden, O. M. Yaghi, *Acc. Chem. Res.* **2008**, *41*, 1782-1789.

[21] In the crystal structures, the positions of Ln atoms in $\mathbf{2}_{\mathbf{Ln}}$ and $\mathbf{3}_{\mathbf{Ln}}$ were found to be different from those of K atoms in K_6[**1**].

[22] V. Baskar, P. W. Roesky, *Dalton Trans.* **2006**, 676-679.

[23] IUPAC. Compendium of Chemical Terminology, 2nd ed. (the "Gold Book"). Compiled by A. D. McNaught and A. Wilkinson. Blackwell Scientific Publications, Oxford (1997). Online version (2019-) created by S. J. Chalk. ISBN 0-9678550-9-8. https://doi.org/10.1351/goldbook.

[24] The contribution of solvated water molecules were excluded in the crystal structure using SQUEEZE in the PLATON software package.[32]

[25] $\mathbf{2}_{\mathbf{La}}$ was converted to $\mathbf{3}_{\mathbf{Lu}}$ by soaking its crystals in 0.1 M aqueous $Lu(OAc)_3$ for one week, which was confirmed by the X-ray fluorescence and single-crystal X-ray analyses. On the other hand, the reverse conversion from $\mathbf{3}_{\mathbf{Lu}}$ to $\mathbf{2}_{\mathbf{La}}$ did not occur when crystals of $\mathbf{3}_{\mathbf{Lu}}$ were soaked in 0.1 M aqueous $La(OAc)_3$ under the same conditions, although the X-ray fluorescence analysis indicated the Lu^{3+}-to-La^{3+} exchange by ~10%.

[26] R. L. Carlin, *Magnetochemistry*, Springer, N.Y., 1986, Chap. 9.

[27] The decrease of $\chi_M T$ values upon cooling is due to the change of the thermal population of m_J microstate of Ln^{3+}.[25]

[28] S.-D. Han, X.-H. Miao, S.-J. Liu, X.-H. Bu, *Chem. Asian J.* **2014**, *9*, 3116-3120.

[29] K. New, C. M. Andolina, J. R. Morrow, *J. Am. Chem. Soc.* **2008**, *130*, 14861-14871.

[30] a) R. Sen, D. K. Hazra, M. Mukherjee, S. Koner, *Eur. J. Inorg. Chem.* **2011**, 2826-2831; b) Y. Zhang, Y. Wang, L. Liu, N. Wei, M.-L. Gao, D. Zhao, Z.-B. Han, *Inorg. Chem.* **2018**, *57*, 2193-2198.

[31] H. Tabe, C. Terashima, Y. Yamada, *Catal. Sci. Technol.* **2018**, *8*, 4747-4756.

[32] A. L. Spek, *Acta Crystallogra.* **2015**, *C71*, 9-18.

Entry for the Table of Contents

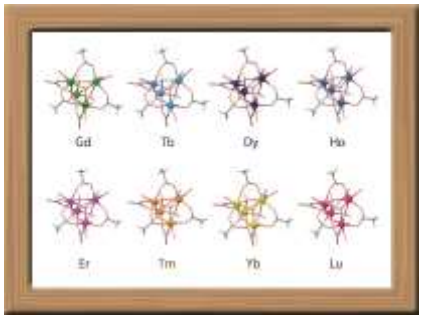

Soaking crystals of $K_6[Rh_4Zn_4O(L\text{-cysteinate})_{12}]$ in a lanthanide acetate solution results in the complete exchange of K^+ with Ln^{3+} in a single-crystal-to-single-crystal process. For late lanthanides (Ln = Gd - Lu), this process afforded a series of lanthanide cubane clusters with a $[Lu_4(\mu_3\text{-}OH)_4]^{8+}$ core, which connect the $Rh^{III}_4Zn^{II}_4$ complex anions in a 3D MOF structure, showing magnetic cooling and heterogeneous catalytic abilities.

Institute and/or researcher Twitter usernames: @osaka_univ, @NobutoYoshinari